



ELSEVIER

Available online at [www.sciencedirect.com](http://www.sciencedirect.com)

SCIENCE @ DIRECT®

Microporous and Mesoporous Materials xxx (2003) xxx–xxx

MICROPOROUS AND  
MESOPOROUS MATERIALS[www.elsevier.com/locate/micromeso](http://www.elsevier.com/locate/micromeso)

## Synthesis and characterization of MCM-41-supported Ba<sub>2</sub>SiO<sub>4</sub> base catalyst

Quanchang Li <sup>a</sup>, Suzanne E. Brown <sup>a</sup>, Linda J. Broadbelt <sup>a,\*</sup>,  
Jian-Guo Zheng <sup>b</sup>, N.Q. Wu <sup>c</sup>

<sup>a</sup> Department of Chemical Engineering, Center for Catalysis and Surface Science, Northwestern University,  
2145 Sheridan Road, Evanston, IL 60208-3120, USA

<sup>b</sup> Department of Materials Science and Engineering, Electron Probe Instrumentation Center, USA

<sup>c</sup> Department of Chemistry, Keck Interdisciplinary Surface Science Center, Northwestern University, Evanston, IL 60208, USA

Received 26 November 2002; received in revised form 20 January 2003; accepted 23 January 2003

### Abstract

A novel MCM-41-supported base catalyst, Ba-MCM-41, was synthesized with a modified impregnation method. Ba<sub>2</sub>SiO<sub>4</sub> was synthesized on the MCM-41 pore wall as confirmed by characterization using X-ray diffraction, X-ray photoelectron spectroscopy, X-ray fluorescence, N<sub>2</sub> adsorption, <sup>29</sup>Si MAS NMR and transmission electron microscopy. It was also demonstrated that a highly ordered Ba-MCM-41 catalyst with high barium loading (4.1–25.2 wt.%) and dispersion was obtained using this method. The basicity of the catalyst, which was characterized according to the binding energy of O 1s, was increased with increasing amounts of barium in the catalyst.

© 2003 Published by Elsevier Science Inc.

**Keywords:** Barium; MCM-41; Barium silicate; Impregnation

### 1. Introduction

The discovery [1,2] of MCM-41 mesoporous molecular sieves has sparked much research into developing new materials with uniform pore size and shape that have very high surface area and adsorption capacity. The development of such materials is of great importance in many areas of modern science and technology [3–6]. These materials are best appreciated in systems where mo-

lecular recognition is needed, e.g., shape-selective catalysis, selective adsorption and separation processes, chemical sensors, and nanotechnology. Ordered mesoporous oxides of the MCM-41 type have been used and evaluated with respect to their catalytic properties as supports, mainly for metal particles or molecular catalysts. However, they might also be useful, with possibly even broader applications, for the preparation of supported base metal oxides that are important in many catalytic reactions [7].

A common method for preparing supported base metal oxides is impregnation, where a porous support is repeatedly dipped into a solution containing a desired catalytic agent. It is often desir-

\* Corresponding author. Tel.: +1-847-491-5351/7398; fax: +1-847-491-3728.

E-mail address: [broadbelt@northwestern.edu](mailto:broadbelt@northwestern.edu) (L.J. Broadbelt).

able to apply the agent uniformly in a predetermined quantity to a preset depth of penetration, but penetration of the liquid solution into the porous support is hindered by air trapped in the pores. In addition, when calcination is employed, the exiting gas will remove the liquid at the exit of the pores, resulting in formation of some catalytic particles on the external surface of the porous material. As a result, several groups [8–10] have reported many small particles that were formed on the external surface of porous materials if conventional impregnation was used to prepare catalysts with metal oxides supported on the surface of a mesoporous material. Generally, various techniques like pressurizing, vacuum treatment, or acoustic activation have been proposed to remove gas trapped in the pores. Therefore, these techniques can be used to modify a typical impregnation method and facilitate the impregnation process.

In the present paper, we report the synthesis of a highly dispersed basic Ba-MCM-41 catalyst by a modified impregnation method which employed reduced pressure. While the preparation of BaO particles supported on MCM-41 has been reported [11], our preparation method resulted in the formation of BaSiO<sub>4</sub> on the framework of MCM-41. To the best of our knowledge, this synthesis of a Ba<sub>2</sub>SiO<sub>4</sub> phase on the framework of MCM-41 was achieved for the first time.

## 2. Experimental

### 2.1. Synthesis

Tetramethylammonium hydroxide (TMAOH), cetyltrimethylammonium bromide (CTMAB), fumed silica and barium nitrate were obtained from Aldrich. Distilled water was used for all syntheses.

The material MCM-41 was synthesized according to the procedure reported in the literature [15]. The molar ratio of the components was as follows: Si:0.25 CTAB:0.2 TMAOH:40 H<sub>2</sub>O. Once the silica was added, the solution was stirred for two hours. The resulting gel was then transferred into a Teflon-lined autoclave and aged at 150 °C for 48 h.

After aging, the gel was filtered, washed several times with distilled water, and dried at room temperature. Once dry, the gel was then calcined at 550 °C (heating rate of 1 °C/min) for 4 h in order to remove the organic template and create the hollow porous structure. The calcined MCM-41 was characterized by low-angle X-ray diffraction (XRD), N<sub>2</sub> sorption and transmission electron microscopy (TEM).

The MCM-41-supported Ba<sub>2</sub>SiO<sub>4</sub> catalyst was first obtained by a modified wet impregnation method. 7.5 g of barium nitrate were dissolved in 100 ml distilled water. 0.9 g MCM-41 were added to the barium nitrate solution. After stirring for 0.5 h under reduced pressure (achieved via water aspiration) at room temperature, the solid was filtered from the solution and dried at room temperature. Final calcination was carried out at 600 °C for 2 h (heating rate of 1 °C/min), and the Ba-MCM-41 catalyst was obtained. Other catalysts containing different amounts of barium were obtained with the same method but varying the barium nitrate concentration (1.0, 2.5, 5.0 g barium nitrate/100 ml H<sub>2</sub>O). These catalysts were fully characterized by XRD, X-ray photoelectron spectroscopy (XPS), X-ray fluorescence (XRF), N<sub>2</sub> sorption, <sup>29</sup>Si MAS NMR and TEM.

### 2.2. Characterization

*X-ray diffraction:* The XRD patterns were collected by a Rigaku DMAX-A diffractometer with CuK $\alpha$  radiation ( $\lambda = 1.5418 \text{ \AA}$ ),  $\theta$ - $2\theta$  geometry and a scintillation detector. Each diffraction pattern was recorded at a step of 0.01° and 1 s per step. All measurements were made at room temperature.

*X-ray photoelectron spectroscopy:* XPS spectra were obtained by using an Omicron ESCA Probe, which was equipped with an electron flood gun. The AlK $\alpha$  radiation (1486.6 eV) was used as an excitation source. The binding energy scale was calibrated with respect to the adventitious carbon (C 1s) at 284.8 eV.

*X-ray fluorescence:* Elemental analysis was carried out on a Bruker S4 Explorer XRF analyzer.

*N<sub>2</sub> sorption:* A Tristar 3000 N<sub>2</sub> sorption apparatus was used to collect the BET data. The sam-

88  
89  
90  
91  
92  
93  
94  
95  
96  
97  
98  
99  
100  
101  
102  
103  
104  
105  
106  
107  
108  
109  
110  
111  
112  
113  
114  
115  
116  
117  
118  
119  
120  
121  
122  
123  
124  
125  
126  
127  
128  
129  
130  
131  
132  
133

134 ples were degassed at 250 °C overnight before the  
 135 measurements were taken. The BET surface area  
 136 was calculated based on the adsorption data in the  
 137 relative partial pressure range of 0.05–0.2. Pore  
 138 size distributions were determined based on the  
 139 Barrett–Joyner–Halender (BJH) adsorption curve.  
 140 <sup>29</sup>Si magic angle spinning (MAS) solid-state  
 141 NMR: <sup>29</sup>Si spectra were recorded on a Varian  
 142 VXR 300 spectrometer using zirconia rotors of 5  
 143 mm in diameter spinning at 4 kHz in air. <sup>29</sup>Si  
 144 NMR spectra were acquired at 59.57 MHz by  
 145 xpolar pulse sequence, with a delay time of 10 s.  
 146 1440 scans were sufficient to give high quality  
 147 spectra. Chemical shifts are given as  $\delta$  from the  
 148 external polydimethylsilane (PDMS) standard.

149 *Transmission electron microscopy*: TEM was  
 150 carried out on a Hitachi HF-2000 TEM, which is  
 151 capable of atomic resolution with a high-brightness  
 152 cold cathode field emission gun operated at 200 kV.  
 153 Samples were prepared by suspending porous ma-  
 154 terials in ethanol followed by sonication for 30 min  
 155 in an ultrasonic bath. The suspension was dropped  
 156 onto a copper grid and allowed to dry.

### 157 3. Results and discussion

158 The MCM-41 host was synthesized with cetyltri-  
 159 methylammonium bromide (CTAB) as the tem-  
 160 plate according to the procedure reported in the  
 161 literature [12]. The calcined MCM-41 was charac-  
 162 terized by low-angle XRD measurements (which  
 163 exhibit the characteristic reflections of high-quality  
 164 hexagonal mesostructures, Fig. 1), N<sub>2</sub> sorption  
 165 studies (Table 1) and TEM (Fig. 2). The Brunauer–  
 166 Emmett–Teller (BET) surface area of the empty  
 167 MCM-41 was 986 m<sup>2</sup>/g, and the pore-size distri-  
 168 bution centered at 3.2 nm was calculated from BJH  
 169 theory on the basis of N<sub>2</sub> adsorption data.

170 For the introduction of barium species onto the  
 171 MCM-41 support, a modified wet impregnation  
 172 method was employed under reduced pressure  
 173 (achieved via water aspiration). As discussed in  
 174 Section 1, gas adsorbed in the MCM-41 pores will  
 175 hinder the deposition of barium nitrate on the pore  
 176 walls. As a result, particles will be deposited on the  
 177 external surface of the MCM-41. To prevent this,  
 178 we used reduced pressure to remove substantial

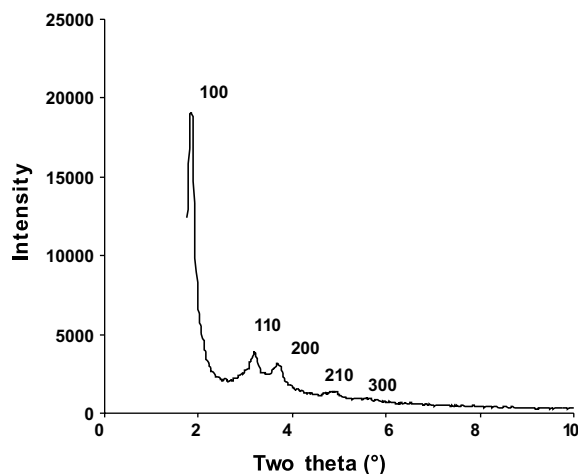


Fig. 1. Powder XRD pattern of the calcined form of MCM-41.

Table 1  
XRF and N<sub>2</sub> adsorption results of MCM-41 and Ba-MCM-41 catalysts

	Barium (wt. %)	S <sub>BET</sub> (m <sup>2</sup> /g)	Pore size (nm)	Pore volume (ml/g)
MCM-41	0	986	3.2	0.947
Ba-MCM-41	4.1	768	3.1	0.705
	8.9	698	3.1	0.638
	15.3	582	3.0	0.526
	25.2	568	3.0	0.516

179 amounts of gas from the pore structure, facilitat-  
 180 ing the penetration of the barium nitrate solution  
 181 in the pores. The solid was filtered from the solu-  
 182 tion and dried at room temperature. Final calci-  
 183 nation was carried out at 600 °C for 2 h (heating  
 184 rate of 1 °C/min), and the Ba-MCM-41 catalyst  
 185 was obtained.

186 To confirm the formation of the Ba<sub>2</sub>SiO<sub>4</sub> phase,  
 187 the calcined catalyst powder with the highest  
 188 barium loading achieved (25.2 wt.% Ba), was  
 189 characterized by XRD (Fig. 3). Fig. 3a and b  
 190 shows the XRD pattern of the MCM-41 supported  
 191 Ba<sub>2</sub>SiO<sub>4</sub> base catalyst in the low-angle region  
 192 ( $2\theta = 1.75\text{--}10^\circ$ ) and the high-angle region  
 193 ( $2\theta = 15\text{--}35^\circ$ ), respectively. It is observed that  
 194 the highly ordered hexagonal pore structure of MCM-  
 195 41 is still intact, while the intensity of the charac-  
 196 teristic XRD reflections of MCM-41 (Fig. 1) is

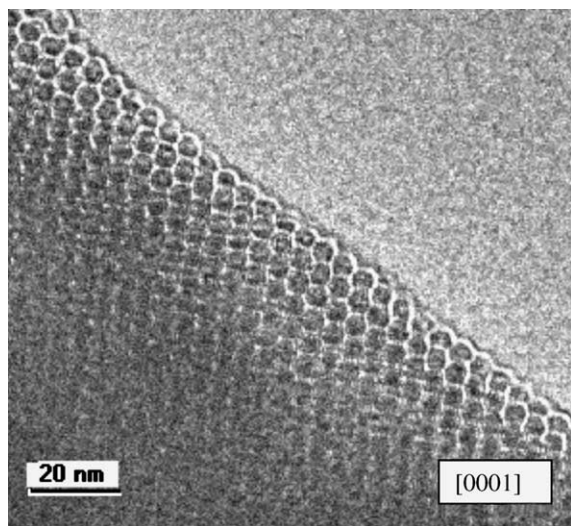


Fig. 2. TEM images of calcined MCM-41 viewed through the pore axis [0001].

197 reduced for the MCM-41 supported  $\text{Ba}_2\text{SiO}_4$  catalyst. This can be attributed to modification of the  
 198 pore wall with  $\text{Ba}_2\text{SiO}_4$ , which reduces the scattering contrast between the pores and the walls of  
 199 the molecular sieve [13]. The tiny reflections ( $2\theta = 26.1^\circ, 29.7^\circ, 30.4^\circ$  and  $30.9^\circ$ ) of the  $\text{Ba}_2\text{SiO}_4$   
 200 phase in the XRD pattern (high-angle region) of the catalyst indicate the formation of  $\text{Ba}_2\text{SiO}_4$ . It is  
 201 noteworthy that there were no clear reflections found in the XRD patterns of the MCM-41 supported  
 202  $\text{Ba}_2\text{SiO}_4$  catalysts in which the Ba content  
 203  
 204  
 205  
 206  
 207

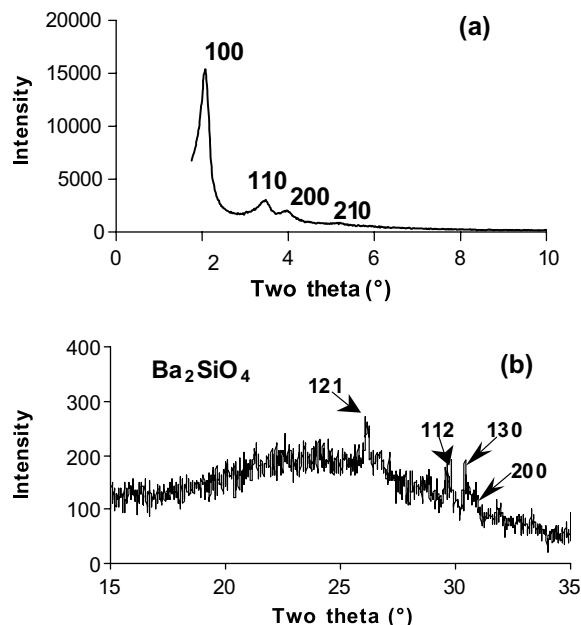


Fig. 3. XRD patterns of the MCM-41-supported  $\text{Ba}_2\text{SiO}_4$  catalyst.

208 was less than 25.2 wt.%. This implies that lower Ba contents will not result in the formation of continuous  
 209 crystalline  $\text{Ba}_2\text{SiO}_4$  on the framework of MCM-41 or that the size of crystalline  $\text{Ba}_2\text{SiO}_4$  is too small to be detected by XRD. It is interesting  
 210 that instead of the (130) plane of the  $\text{Ba}_2\text{SiO}_4$  phase, the (121) plane shows the highest reflection peak in the XRD pattern (Fig. 4b) [14]. This may  
 211  
 212  
 213  
 214  
 215

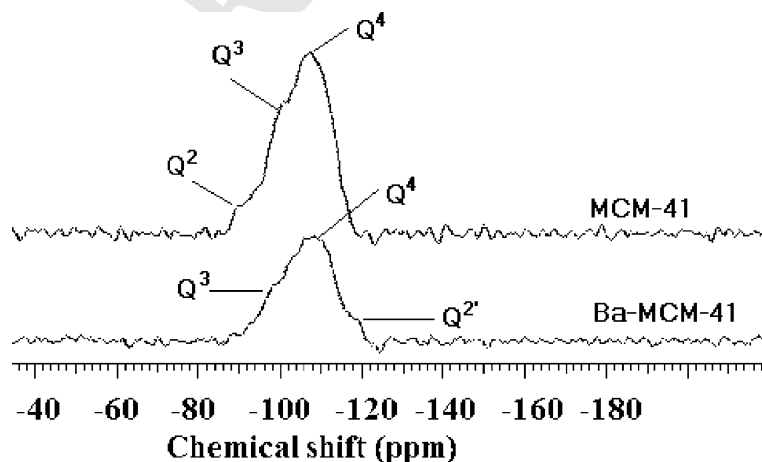


Fig. 4.  $^{29}\text{Si}$  solid-state MAS NMR of pure MCM-41 and the MCM-41-supported  $\text{Ba}_2\text{SiO}_4$  catalyst.

216 be due to MCM-41 limiting the growth of the  
217  $\text{Ba}_2\text{SiO}_4$  phase and the (1 2 1) plane growing on the  
218 pore wall along the axis of the hexagonal pores of  
219 MCM-41.

220 Evidence of the  $\text{Ba}_2\text{SiO}_4$  phase, which formed  
221 during the modification of the silica MCM-41  
222 surface, was also obtained from magic angle  
223 spinning (MAS) solid-state  $^{29}\text{Si}$  NMR (Fig. 4).  
224 Three different coordinations of Si,  $\text{Q}^4$  (Si-nuclei  
225  $(\text{OSi})_4$ ),  $\text{Q}^3$  (Si-nuclei  $(\text{OSi})_3(\text{OH})$ ) and  $\text{Q}^2$  (Si-nuclei  
226  $(\text{OSi})_2(\text{OH})_2$ ), were found at  $-108$ ,  $-101$  and  $-92$   
227 ppm in the spectrum of pure MCM-41, which is in  
228 agreement with literature results [15]. After modi-  
229 fication of the MCM-41 surface by Ba impregna-  
230 tion, the  $\text{Q}^2$  species peak shifts from  $\delta = -92$  to  
231  $-119$  ppm. This is because the surface hydroxyl  
232 groups of the  $\text{Q}^2$  (Si-nuclei  $(\text{OSi})_2(\text{OH})_2$ ) species  
233 reacted with the barium source and formed the  $\text{Q}^{2'}$   
234 (Si-nuclei  $(\text{OSi})_2\text{O}_2\text{Ba}$ ) species at  $-119$  ppm.

235 TEM images of the MCM-41 supported  
236  $\text{Ba}_2\text{SiO}_4$  catalyst (25.2 wt.% Ba) are shown in Fig.  
237 5. These images reveal that the hexagonally order-  
238 ed mesostructure of the MCM-41 host material  
239 was unaffected by surface modification with  
240  $\text{Ba}_2\text{SiO}_4$ . No crystalline particles were found on  
241 the external surface of the MCM-41 framework,  
242 indicating that all barium sources were dispersed  
243 inside the mesostructure homogeneously. The  
244 TEM images also show a much stronger contrast  
245 than the pure silica MCM-41 (Fig. 2), which might  
246 be partially attributed to the presence of barium as  
247 a stronger scatterer/absorber in a homogeneous  
248 distribution.

249  $\text{N}_2$  adsorption results (Table 1) show that the  
250 BET surface area is still above  $568 \text{ m}^2/\text{g}$  when the  
251 barium content was increased to 25.2 wt.%, and  
252 the average pore size decreases from 3.2 to 3.0 nm  
253 due to the formation of  $\text{Ba}_2\text{SiO}_4$  on the pore walls.  
254 In comparison to literature results [11] in which  
255 only 10% by weight BaO particles formed in the  
256 porous structure, the deposition of BaO clusters  
257 reduced the pore space, resulting in a decrease of  
258 the BET surface area from 982 to  $535 \text{ m}^2/\text{g}$ . The  
259 decrease in our surface area was comparable for a  
260 significantly higher Ba content, suggesting that the  
261 modified impregnation method more successfully  
262 dispersed Ba on the framework of MCM-41. This  
263 might be due to the use of a vacuum system that

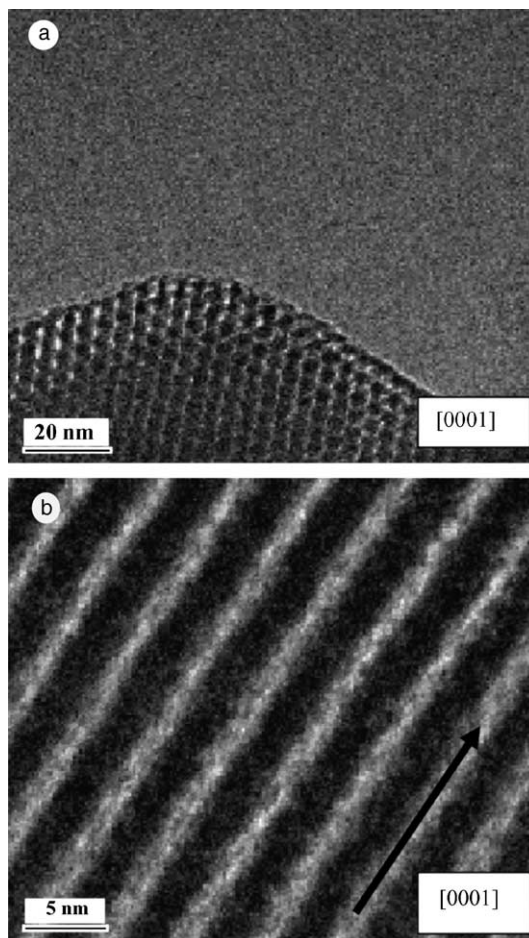


Fig. 5. TEM images of calcined Ba-MCM-41 catalyst viewed (a) through the pore axis [000 1] and (b) along the pore channels ([000 1] direction depicted by arrow).

264 helped remove all of the gas from the porous  
265 structure of MCM-41 and the use of a barium  
266 nitrate solution that dispersed Ba into MCM-41  
267 homogeneously before calcination.

268 XPS measurements were carried out on the  
269 MCM-41-supported  $\text{Ba}_2\text{SiO}_4$  catalyst to confirm  
270 the formation of barium silicate and to determine  
271 the surface basicity. Fig. 6a shows the Si 2p bind-  
272 ing energy in both MCM-41 and  $\text{Ba}_2\text{SiO}_4$ . The full  
273 width at half maximum of the Si 2p peaks in-  
274 creased with increasing Ba content, and the degree  
275 of asymmetry also increased. Deconvolution of the  
276 peaks through fitting revealed two distinct Si 2p

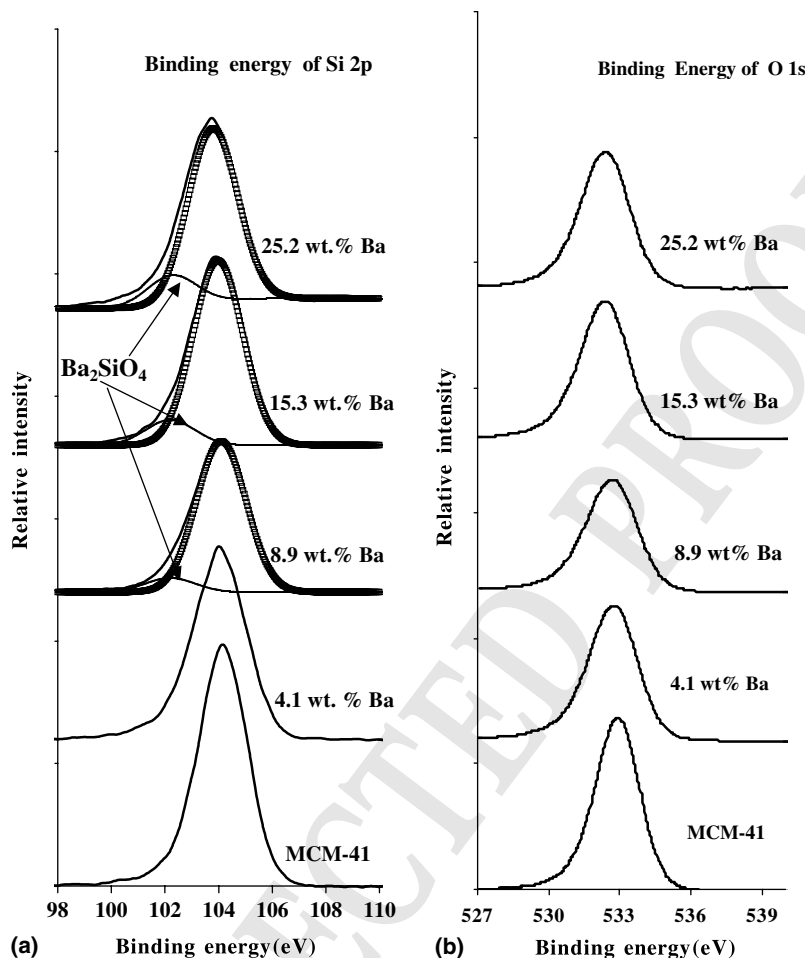


Fig. 6. XPS spectra of pure MCM-41 and the MCM-41-supported  $\text{Ba}_2\text{SiO}_4$  base catalyst focusing on: (a) Si 2p and (b) O 1s peaks.

277 binding energy peaks, indicating the existence of  
 278 two different Si species: the main peak at 104.1 eV  
 279 is attributed to the  $\text{SiO}_2$  of MCM-41, while the  
 280 other small peak at 102.2 eV likely arises from the  
 281 new  $\text{Ba}_2\text{SiO}_4$  species. In addition, XPS spectra also  
 282 provide very important information about changes  
 283 in the surface basicity (Fig. 6b). Since the binding  
 284 energy of O 1s decreases from 533.0 to 532.5 eV  
 285 after formation of  $\text{Ba}_2\text{SiO}_4$  on the framework of  
 286 MCM-41, this means that the Lewis basicity of the  
 287 surface increased after the modification of MCM-  
 288 41 with  $\text{Ba}_2\text{SiO}_4$ .

#### 4. Conclusions

290 Although ordered mesoporous MCM-41 mate-  
 291 rials have been used and evaluated with respect to  
 292 their catalytic properties as supports, the work  
 293 reported in those publications [7,10,11,13,16] was  
 294 undertaken with the goal of creating highly dis-  
 295 persed oxide species using ordered mesoporous  
 296 supports. The synthesis of a highly dispersed basic  
 297 species,  $\text{Ba}_2\text{SiO}_4$ , on the framework of MCM-41 is  
 298 reported for the first time to the best of our  
 299 knowledge. The combined results of XRD, XPS,  
 300 XRF, TEM, MAS NMR and  $\text{N}_2$  adsorption have  
 301 confirmed the existence of a  $\text{Ba}_2\text{SiO}_4$  phase on the

289

290  
291  
292  
293  
294  
295  
296  
297  
298  
299  
300  
301

302 framework of MCM-41. The catalyst basicity  
303 could be improved by changing the Ba content of  
304 the catalysts. Further investigations of the process  
305 of surface modification of MCM-41 with different  
306 basic species and catalytic applications of these  
307 materials are underway.

### 308 Acknowledgements

309 The authors are grateful for the support of the  
310 CAREER Program of the National Science  
311 Foundation (CTS-9623741). Prof. Snurr and Prof.  
312 Kung are acknowledged for offering laboratory  
313 equipment. Dr. Kai Zhang is acknowledged for  
314 helpful discussions on XRD.

### 315 References

- 316 [1] C.T. Kresge, M.E. Leonowicz, W.J. Roth, J.C. Vartuli, J.S.  
317 Beck, *Nature* 359 (1992) 710.
- 318 [2] J.S. Beck, J.C. Vartuli, W.J. Roth, M.E. Leonowicz, C.T.  
319 Kresge, K.D. Schmitt, C.T.W. Chu, D.H. Olson, E.W.  
320 Sheppard, S.B. McCullen, J.B. Higgins, J.L. Schlenker, J.  
321 *Am. Chem. Soc.* 114 (1992) 10834.
- [3] T.J. Barton, L.M. Bull, W.G. Klemperer, D.A. Loy, B. 322  
McEnaney, M. Misono, P.A. Monson, G. Pez, G.W. 323  
Scherer, J.C. Vartuli, O.M. Yaghi, *Chem. Mater* 11 (1999) 324  
2633. 325
- [4] Y. Ma, W. Tong, H. Zhou, L. Suib, *Micropor. Mesopor.* 326  
*Mater.* 37 (2000) 243. 327
- [5] K. Cheetham, G. Férey, T. Loiseau, *Angew. Chem. Int.* 328  
*Ed. Engl* 38 (1999) 3269. 329
- [6] P. Behrens, *Adv. Mater.* 5 (1993) 127. 330
- [7] F. Schüth, A. Wingen, J. Sauer, *Micropor. Mesopor.* 331  
*Mater.* 44–45 (2001) 465. 332
- [8] A. Bourlinos, A. Simopoulos, N. Boukos, D. Petridis, J. 333  
*Phys. Chem. B* 105 (2001) 7432. 334
- [9] D. Lensveld, J. Mesu, A. Dillen, K. Jong, *Micropor.* 335  
*Mesopor. Mater.* 44–45 (2001) 401. 336
- [10] R.S. Mulukutla, K. Asakura, T. Kogure, S. Namba, Y. 337  
Iwasawa, *Phys. Chem. Chem. Phys.* 1 (1999) 2027–2032. 338
- [11] S. Jaenicke, G.K. Chuah, X.H. Lin, X.C. Hu, *Micropor.* 339  
*Mesopor. Mater.* 35–36 (2000) 143. 340
- [12] R. Mokaya, *J. Phys. Chem. B* 104 (2000) 8279–8286. 341
- [13] B. Marler, U. Oberhagemann, S. Vortmann, H. Gies, 342  
*Micropor. Mesopor. Mater.* 6 (1996) 375. 343
- [14] H. Uchikawa, K. Tsukiyama, *ISIS Annual Report* 73 344  
(1965) 106. 345
- [15] B.H. Wouters, T. Chen, M. Dewilde, P.J. Grobet, *Micro-* 346  
*por. Mesopor. Mater.* 44–45 (2001) 453–457. 347
- [16] T. Abe, Y. Tachibana, T. Uematsu, M. Iwamoto, *J. Chem.* 348  
*Soc. Chem. Commun.* (1995) 1617. 349